

## Mechanical properties of stanene

TAO Lele<sup>1</sup>, LU Pengfei<sup>1</sup>, YANG Chuanghua<sup>2</sup>, WU Liyuan<sup>1</sup>, SU Rui<sup>3</sup>

(1. State Key Laboratory of Information Photonics and Optical Communications, Beijing  
University of Posts and Telecommunications, Beijing 100876;

2. School of Physics and Telecommunication, Shaanxi University of Technology, Hanzhong,  
Shaanxi 723001;

3. Beijing Computational Science Research Center, Beijing 100084)

**Abstract:** Elastic properties of stanene under equiaxial and uniaxial tensions along armchair as well as zigzag directions were investigated by first-principles calculations. The stress-strain relation was calculated. The relaxation of the internal atom's position was analyzed. The high order elastic constants were calculated by fitting the polynomial expressions. The Young's modulus and Poisson ratio of the stanene was calculated to be 24.14 N/m and 0.39, respectively. The stanene exhibits lower Young's modulus than those of the proceeding Group IV elements, which is attributed to the smaller sp<sup>2</sup>-sp<sup>3</sup> bond energy in stanene than those of silicene and germanene. Calculated values of ultimate stresses and strains, second order elastic constants, and the in-plane Young's modulus are all positive. All of these described above may prove that stanene is mechanically stable.

**Key words:** mechanics of materials; Stanene; Bond length evolution; Stress-strain responses

### 0 Introduction

The low-dimensional materials, such as quantum dots, nanowire, and graphene, have attracted much interest in recent decades. As a form of two-dimensional (2D) carbon, graphene has shown its potential inspirations in the applications of nanoelectronics and solar cells<sup>[1-4]</sup>. In order to overcome the zero bandgap property of graphene, 2D materials<sup>[5-10]</sup>, such as transition metal dichalcogenides (TMDs), metal monochalcogenides, silicene and germanene have also been reported to extend their applications in the next-generation electronic and optoelectronic devices.

Tin is a group-IV element which shows strong spin-orbit coupling (SOC) effect on the band structure. The chemical symbol of tin is Sn, originating from the Latin word "stannum" for tin<sup>[11]</sup>. Stanene is a 2D monolayer consists of Sn atoms which are arranged in a manner similar to the graphene. Stanene as well as its derivative structures have been expected to be highly valuable in both scientific and engineer views and several experimental and theoretical works have been reported. These works covers both thermal stability and the electron structure of the stanene. In a preprint paper by Zhu et al.<sup>[12]</sup>, the 2D stanene was fabricated for the first time by the molecular beam epitaxy technique. The atomic and electronic structures determined by scanning tunneling microscopy and angle-resolved photoemission spectroscopy provides researchers a new insight on the previous theoretical works. Theoretically, B.Broek et al.<sup>[13]</sup> studied the structural, mechanical and electronic properties of stanene. They explored applied electric field and applied strain as functionalization mechanisms allows for an induced bandgap up to 0.21 eV. In a recent work, Chou et al.<sup>[14]</sup> found hydrogenation of 2 to 4 bilayer films results in a non-trivial topological insulators (TIs) phase. Xu et al.<sup>[11]</sup> found that the quantum-spin Hall (QSH) states can be effectively tuned by applying external strains. However, unlike graphene, stanene without hydrogenation does not show a zero-gap band structure. Thus the hydrogenation induced gap opening of about 0.3 eV promises the TI properties in a temperature range up to 373.15K which is of great importance for integrated circuits applications.

Mechanical properties are significant for manufacturing 2D nanomaterials devices. Strain engineering is an important method to study the structural and functional properties of 2D materials<sup>[15]</sup>.

Foundations: the National Basic Research Program of China (973) Grant (No.2014CB643900);the National Natural Science Foundation of China Grant (No.61440061)

Brief author introduction:LU Pengfei (1976-),Male,Associate professor,Research on physical property of the nanometer photoelectron materials. E-mail: photon@bupt.edu.cn

Because of thickness of monolayer, stanene will be exposed to strain by the mismatch of lattices on a substrate. Therefore, it is important to understand the tension-induced mechanical property of stanene, including ultimate strength, nonlinear elastic properties, and strain energy. The main motivation of this paper is to study the linear and nonlinear mechanical properties of stanene, and present a description of the elastic properties based on ab initio density functional theory calculations.

## 1 METHODS AND MODELS

Our first-principles calculations are based on the density-functional theory (DFT) as implemented in the Vienna ab initio Simulation Package (VASP)<sup>[16]</sup>. The exchange-correlation potentials were approximated by GGA in the Perdew-Burke-Ernzerhof (PBE) form. A plane-wave basis set was employed within the framework of the projector augmented wave (PAW) method. The hexagonal structures were optimized by using periodically repeating supercell having hexagonal lattice in 2D, and the height of the supercell was maintained at 10Å for eliminating the interactions between crystal lattice. The kinetic-energy cutoff of the plane wave was set to be 250 eV. The convergence in force and energy was set as 10<sup>-3</sup> eV/Å and 10<sup>-6</sup> eV/Å, respectively. The k-point was employed with (34×17) Monkhorst-Pack in the Brillouin zone. The models are shown in Fig.1. In Fig.1 (a), top view of stanene is presented and the model we use to calculate is shown in red square (4 atoms); Fig.1 (b) is the sideview of supercell.

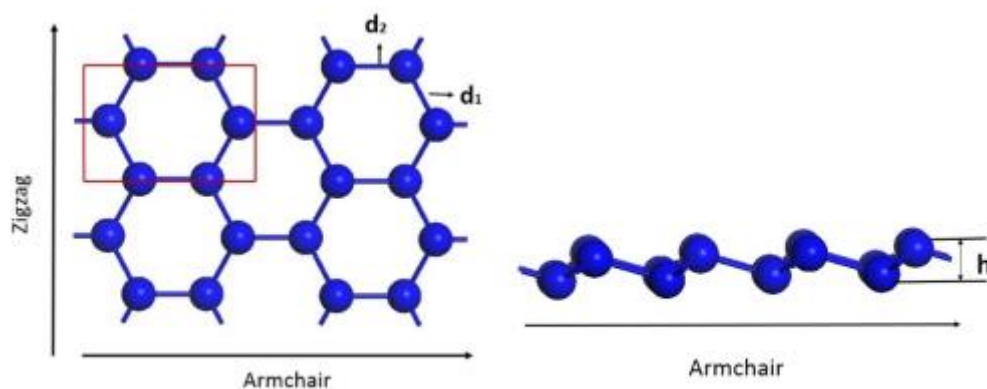


Fig.1 Atomic structure of stanene. (a) top view of stanene (b) side view of stanene.

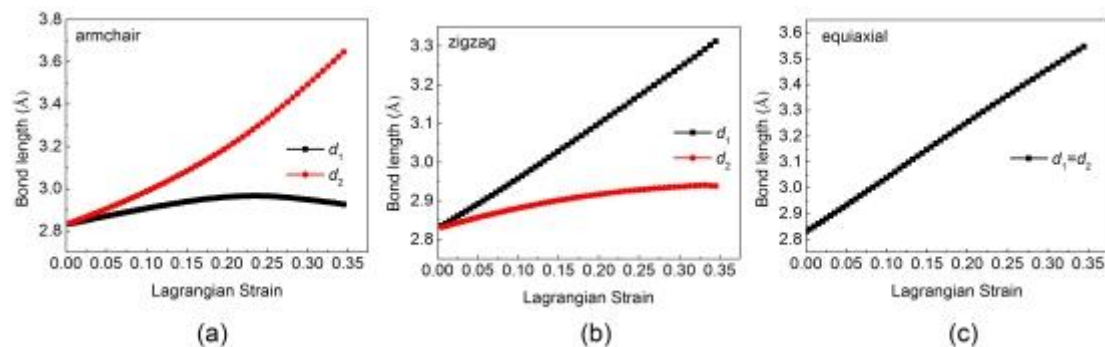
## 2 RESULTS AND DISCUSSION

### 2.1 Structural properties of stanene

In this work, internal atoms position relax along the Lagrange strain is presented. The reference strain-free structure is set to the most energetically favorable structure. A series Lagrange strain with the amplitude changing from 0.5% to 40% is then imposed on stanene. Three kinds of tensions, such as AC, ZZ and EQ, are introduced and all atoms under the three types of tensions are fully optimized. The changes of the three structure parameters:  $d_1$ ,  $d_2$  and  $d_3$  are plotted in Fig. 2 and Fig.3, respectively. The  $d_1$  and  $d_2$  refers to the Sn-Sn bond lengths while the  $d_3$  refers to the height of stanene in wrinkle form. The bond length  $d_1/d_2$  of Sn-Sn is 2.83 Å; while the  $d_3$  is found to be 0.85 Å after the structural optimization.

As shown in Fig.2, when the AC tension is applied, the bond length of  $d_1$  of stanene reaches a maxima of 2.964 Å at the strain of 0.232; while the bond length of  $d_2$  keeps an unlinear increasing against the increased strain. When the ZZ tension is applied, the bond  $d_2$  of stanene is perpendicular to

the direction of tension, and reaches its maximum value of 2.941 Å at the strain of 0.332; while the bond length of  $d_1$  linearly increases with the applied strain. When the EQ tension is applied on stanene, the lengths of bond  $d_1$  and  $d_2$  are equal and linearly increase with the increasing strain.

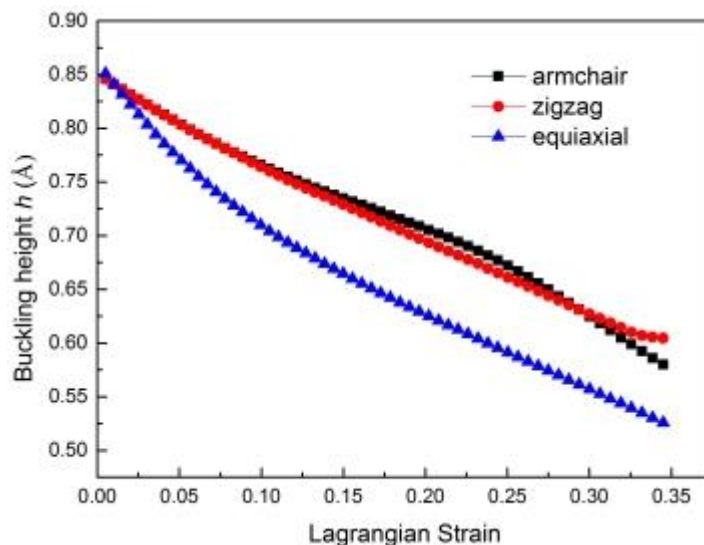


85

Fig.2 Bond length evolution of  $d_1$  and  $d_2$  in (a)AC, (b)ZZ, and (c)EQ directions

Figure.3 shows the variation of  $d_3$  in stanene. The height of wrinkle is an important index to describe the surface configuration. The tension imposed on stanene will decrease the height of  $d_3$ . The curves for AC and ZZ tensions are almost identical in the harmonic region. With the increasing strain from 0.12 to 0.35, the anisotropic properties become more and more obvious. When the EQ tension is applied,  $d_3$  will decrease more quickly compared the effect of other two tensions.

90



95

Fig.3 The evolution of buckling height  $h$  under three type of strains

## 2.2 Strain energy

Strain energy is introduced to describe the system's deformations under tension. Strain energy of per atom was defined as  $E_s = (E_{tot} - E_0)/n$ <sup>[17]</sup>. Here  $E_{tot}$  is the total energy of the strained system,  $E_0$  is the total energy of the strain-free system, and  $n$  is the number of atoms in the unit cell.  $E_s$  of stanene as a function of strain in three types are shown in Fig.4. It can be seen that  $E_s$  is anisotropic with strain direction. The harmonic region where the  $E_s$  is a quadratic function of applied strain can be obtained between  $0 < \epsilon < 0.02$ . In the harmonic region, the strain energy density are linearly increasing with the increase of strains. With the increasing of strain, the system will be located at the anharmonic region.

100

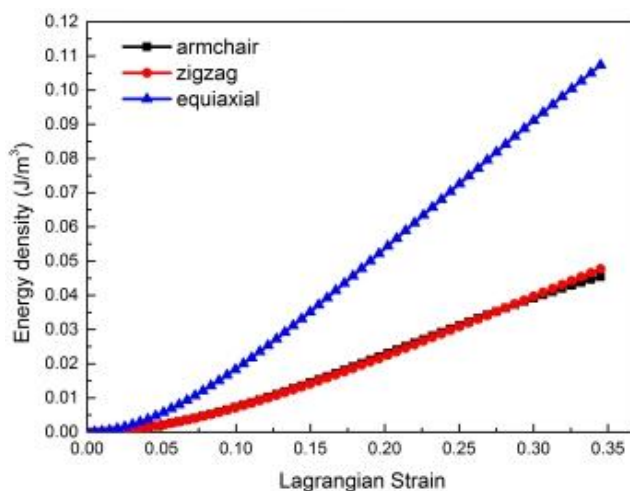
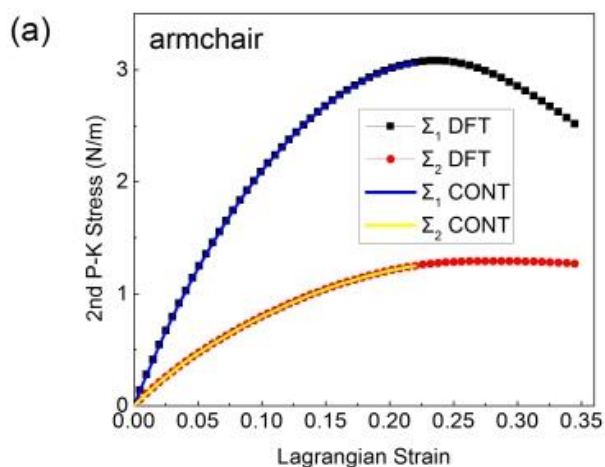


Fig.4 Energy density's change of Lagrangian strain at three direction

### 2.3 Strain-Stress curves

The ultimate strain is determined by the intrinsic bonding strengths and acts as a lower limit of the critical strain. With even larger loading of strains, the systems will undergo irreversible structural changes, and the systems are in a plastic region where they may fail<sup>[18]</sup>. Beyond the ultimate strains, the stanene under strains are in a meta-stable state, which can be easily damaged by vacancy defects and high temperature effects.

The second P-K stress versus Lagrangian strain relationship for strains along the AC, ZZ and EQ directions are shown in Fig.5. Blue and yellow in Fig. 5(a) and (b) is the result of fit and red and black is the result of the ab-initio calculation. The anharmonic region is the range of strain where the linear stress-strain relationship is invalid and higher order terms are not negligible. The ultimate strength is defined to be the maximum stress where a material can tolerate in the stretching state; while the corresponding strain is the ultimate strain<sup>[18]</sup>. When the strain is imposed on the AC direction, the ultimate strain is 0.24; while the corresponding ultimate strength is 3.08 N/m. In the ZZ direction, d1 is stretched more severely than that in AC direction. The ultimate strength is 3.50 N/m at the ultimate strain of 0.36. However, the ultimate strength is 2.83 N/m with a corresponding ultimate strain of 0.22, and lower than those in AC and ZZ directions. Both the strength and toughness of stanene along the ZZ direction are largest. Below the ultimate strain, the data will be used to determine the high order elastic constants.



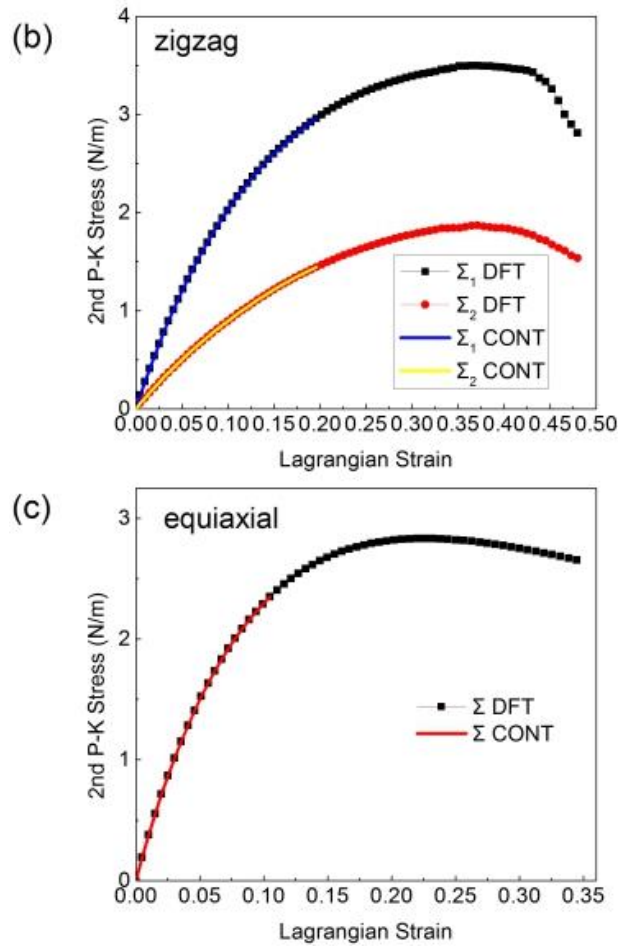


Fig.5 Stress-strain responses of monolayer tin under (a) Armchair (b) Zigzag (c) Equiaxial tensions

### 2.4 Elastic constants

Nonlinear elasticity of stanene can be expressed by high order elastic constants, which reflects the high order nonlinear bond strength under large strains. All fourteen elastic constants appear in the stress-strain relationships for the three special cases collectively (Eq.(8), Eq.(9), Eq.(12), Eq.(13), and Eq.(16)). The values of the elastic constants can be determined by fitting these equations to the DFT results as illustrated in Fig. 5. The dependent nonzero components of SOEC, TOEC, FOEC, and FFOEC are summarized in Table 1.

Higher order (>2) elastic constants are important quantities for studying the properties of 2D materials, such as nonlinear elasticity, thermal expansion, harmonic generation, phonon-phonon interactions, lattice defects, phase transitions, strain softening, and so on. The components of the TOEC and FFOEC tensors are all negative, which ensures that the elastic stiffness softens with strain up to ultimate strain.

Table.1 Nonzero independent components for the SOEC, TOEC, FOEC, and FFOEC tensor components.

SOEC (N/m)	TOEC (N/m)	FOEC (N/m)	FFOEC (N/m)
$C_{11}=28.6$	$C_{111}=-241.3$	$C_{1111}=1469.1$	$C_{11111}=-7668.7$
$C_{12}=11.3$	$C_{112}=-63.2$	$C_{1112}=541.5$	$C_{11112}=-4116.7$
	$C_{222}=-186.4$	$C_{1122}=683.0$	$C_{11122}=-4123.5$
		$C_{2222}=1088.6$	$C_{12222}=-6538.3$
			$C_{22222}=-6913.7$

The in-plane Young's modulus  $Y_s$  and Poisson's ratio  $\nu$  can be solved and got  $Y_s = 24.14$  N/m, and  $\nu = 0.395$  for stanene respectively. The positive values of ultimate tension and the in-plane Young's modulus will indicate that stanene is mechanically stable. Our work could contribute to understand the mechanical properties of stanene if can be tested by experiment. Under large hydrostatic pressure, it is useful to describe the nonlinear elastic properties of materials by the pressure dependent elastic constants<sup>[18,19]</sup>. When pressure was applied, the pressure dependent second-order elastic constants and corresponding derivatives with pressure can be obtained from  $C_{11}$ ,  $C_{12}$ ,  $C_{111}$ ,  $C_{112}$ ,  $C_{222}$ ,  $Y_s$ , and  $\nu$  in Table 1. Our calculated values could be compared with those of experimental study in the near future.

Table.2 Comparison of different materials' elastic constants and passion ratio.

	$C_{11}$ (N/m)	$C_{12}$ (N/m)	$C_{111}$ (N/m)	$C_{112}$ (N/m)	$C_{222}$ (N/m)	$Y_s$ (N/m)	$\nu$
Graphene [19]	352.0	63.6	-3089.7	-453.8	-2928.1	340.8	0.18
Silicene [10]	68.9	23.3	-347.7	-23.1	-270.1	62	0.33
Germanene [10]	47.3	16.7	-439.3	-108.3	-396.4	41.4	0.35
Stanene	28.6	11.3	-241.3	-63.2	-186.4	24.14	0.39

In Table 2, the SOECs and the TOECs of stanene was listed. Corresponding values for graphene, silicene, and germanene are shown for comparison. We have estimated the numerical uncertainty on the values of the elastic constants, and fifth-order fitting has better numerical certainty. In Ref.<sup>[20]</sup>, Modarresi *et al.* obtained that the Young's modulus of stanene was 40 N/m, which was almost equal to that of germanene of 41.4 N/m. Modarresi *et al.* considered the biaxial strain, and the expression of Young's modulus is adopted. However, the calculation of  $Y_s$  should be used the energy vs Lagrangian strain  $\eta$  relationship in order to improve the accuracy. Table 2 obviously shows that the second order elastic constants decrease with the increase of atomic number in group IVA, while Poisson's ratio reverses and Young's modulus of stanene is the smallest. Our calculations conclude that stanene is easier to be deformed. The feature is more conducive to tune the electronic properties of stanene by strain. This is due to the more delocalized outer shell electrons and the larger atomic radius of Sn compare to Si and Ge, which will significantly reduce the energy of Sn-Sn bond (ie. Sn-Sn  $sp^2$ - $sp^3$  puckering). Calculated values of ultimate stresses and strains, second order elastic constants, and the in-plane Young's modulus are all positive. It proves that stanene is mechanically stable. The hydrostatic terms are smaller which means stanene is softer; and shear terms are smaller which will contribute to high compressibility of stanene.

### 3 Conclusion

Tension-induced mechanical properties of stanene were studied by the first-principles DFT calculations. The ultimate strengths of stanene under AC, ZZ and EQ tensions are 3.079 N/m, 3.496 N/m, and 2.83 N/m, respectively. The total fourteen nonzero independent nonlinear elastic constants of stanene were obtained by combining continuum elasticity theory and the homogeneous deformation method. Young's modulus, Poisson's ratio and second-order elastic moduli were calculated out as well. Our work may contribute to the profound understanding of the mechanical properties of stanene.

### References

- [1] C.LEE, X.WEI, J.W.KYSAR AND J.HONE Measurement of the elastic properties and intrinsic strength of monolayer graphene [J] Science,2008,321(5887) :385-388.  
 [2] A.H.CASTRO, F.GUINEA, N.M.R.PERES, K.S.NOVOSELOV AND A.K.GEIM The electronic properties of

- 180 graphene [J].Rev.Mod.Phys.,2009,81 (1):109-162.  
[3] F.SCHWIERZ Graphene transistors[J],Nature Nanotechnology,2010,5(7):487-496.  
[4] J.BARINGHAUS, M.RUAN, F.EDLER, A.TEJEDA, M.SICOT, A.TALEB-IBRAHIMI, A.LI, Z.JIANG, E.H.CONRAD, C.BERGER, C.TEGENKAMP AND W.A.HEER Exceptional ballistic transport in epitaxial graphene nanoribbons[J],Nature,2014,506(7488):349-354.
- 185 [5] Y.ZHANG, Q.JI, J.JU, H.YUAN, J.SHI, T.GAO, D.MA, M.LIU, Y.CHEN, X.SONG, H.Y.HWANG, Y.CUI AND Z.LIU Controlled Growth of High-Quality Monolayer WS<sub>2</sub> Layers on Sapphire and Imaging Its Grain Boundary[J],Acs Nano,2013,7(10):8963-8971.  
[6] R.C.COOPER, C.LEE, C.A.MARIANETTI, X.WEI, J.HONE, J.W.KYSAR Nonlinear elastic behavior of two-dimensional molybdenum disulfide[J],Phys.Rev.B,2013,87(3).
- 190 [7] BEHERA AND G.MUKHOPADHYAY Tailoring the structural and electronic properties of a graphene-like ZnS monolayer using biaxial strain[J],J.Phys.D: Appl. Phys.,2014,47(7).  
[8] D.J.LATE, B.LIU, J.LUO, A.YAN, H.MATTE, M.GRAYSON, C.RAO, V.P.DRAVID GaS and GaSe Ultrathin Layer Transistors[J],Adv. Mater.,2012,24(26):3549-3554.  
[9] S.CAHANGIROV, M.TOPSAKAL, E.AKTÜRK, H.SAHIN AND S.CIRACI Two- and One-Dimensional Honeycomb Structures of Silicon and Germanium[J],Phys. Rev. Lett.,2009,102(23).
- 195 [10] H.ZHANG, R.WANG The stability and the nonlinear elasticity of 2D hexagonal structures of Si and Ge from first-principles calculations[J],Physica B,2011,406(21): 4080-4084.  
[11] Y.XU, B.YAN, H.ZHANG, J.WANG, G.XU, P.TANG, DUAN AND S.ZHANG Large-Gap Quantum Spin Hall Insulators in Tin Films[J],Phys. Rev. Lett.,2013,111(13).
- 200 [12] F.ZHU, W.CHEN, Y.XU Epitaxial growth of two-dimensional stanene[OL].[15 April 2015].http://www.nature.com/nmat/journal/v14/n10/abs/nmat4384.html  
[13] B.BROEK, M.HOUSSA, E.SCALISE, G.POURTOIS, V.AFANAS AND A.STESMANS Two-dimensional hexagonal tin: ab initio geometry, stability, electronic structure and functionalization[J],2D Materials,2014,1(2).  
[14] B.CHOU Hydrogenated ultra-thin tin films predicted as two-dimensional topological insulators[J],New J. Phys.,2014,16.
- 205 [15] G.GUI, J.LI, J.ZHONG Band structure engineering of graphene by strain: First-principles calculations[J],Phys.Rev.B,2008,78(7).  
[16] J.ZHOU, R.HUANG Internal lattice relaxation of single-layer graphene under in-plane deformation [J],J.Mech.Phys.Solids,2008,56(4):1609-1623.
- 210 [17] X.WEI, B.FRAGNEAUD, C.A.MARIANETTI, J.W.KYSAR Nonlinear elastic behavior of graphene: Ab initio calculations to continuum description[J],Phys.Rev.B,2009,80(20).  
[18] Q.PENG, W. JI AND S.DE Mechanical properties of graphyne monolayers: a first-principles study[J],Phys. Chem. Chem. Phys.,2012,14(38):13385-13391.  
[19] Q.PENG, W. JI AND S.DE Mechanical properties of the hexagonal boron nitride monolayer: Ab initio study[J],Comput. Mater. Sci.,2012,56:11-17.
- 215 [20] MODARRESI.M, KAKOEE.A, MOGULKOC.Y Effect of external strain on electronic structure of stanene[J],Comput. Mater. Sci.,2015,101:164-167.

## 锡烯的力学性质研究

- 220 陶乐乐<sup>1</sup>, 芦鹏飞<sup>1</sup>, 杨创华<sup>2</sup>, 伍利源<sup>1</sup>, 苏锐<sup>3</sup>  
(1. 北京邮电大学信息光子学与光通信研究院, 北京 100876;  
2. 陕西理工大学物理与电信工程学院, 陕西汉中 723001;  
3. 北京计算科学研究中心, 北京 100084)

225 **摘要:** 锡烯的弹性性质可以在等轴,之字方向,扶手方向三个方向上施加应力并用第一性原理计算得到.计算得到了应力应变关系,并分析了原子位置的变动.通过多项式得到了高阶弹性常数.得到锡烯的杨氏模量为 24.14N/m 和泊松比为 0.39,锡烯的杨氏模量比同族元素的杨氏模量要小,是由于 sp<sup>2</sup>-sp<sup>3</sup> 轨道间的结合能要比硅烯锗烯的小.计算得到了最大应变应力,二阶弹性常数,杨氏模量是正的,可以表明锡烯是稳定的.

230 **关键词:** 材料力学; 锡烯; 键能突变; 应力应变关系  
中图分类号: O341